Contents lists available at ScienceDirect

BBA - Biomembranes

journal homepage: www.elsevier.com

Changes in biophysical membrane properties induced by the Budesonide/Hydroxy-β-cyclodextrin complex

Andreia G. dos Santos[a, b, 1], Jules Bayiha[a, 1], Gilles Dufour[c], Didier Cataldo[d], Brigitte Evrard[c], Liana C. Silva[b], Magali Deleu[e], Marie-Paule Mingeot-Leclercq[a, *]

[a] *Université catholique de Louvain, Louvain Drug Research Institute, Cellular and Molecular Pharmacology Unit, Avenue E. Mounier 73, B1.73.05, B-1200 Bruxelles, Belgium*
[b] *Universidade de Lisboa, Faculdade de Farmácia, iMed.ULisboa - Research Institute for Medicines, Av. Prof. Gama Pinto, 1649-003 Lisboa, Portugal*
[c] *Université de Liège, Laboratoire de Technologie Pharmaceutique et Biopharmacie, Avenue de l'Hôpital 3, B-4000 Liège, Belgium*
[d] *Université de Liège, CHU, Laboratory of Tumor & Development Biology of the Groupe Interdisciplinaire de Génoprotéomique Appliquée, Avenue de l'Hôpital 3, B-4000 Liège, Belgium*
[e] *Université de Liège, Gembloux Agro Bio-Tech, Laboratoire de Biophysique Moléculaire aux Interfaces, Passage des Déportés, 2, B-5030 Gembloux, Belgium*

ARTICLE INFO

Article history:
Received 10 February 2017
Received in revised form 1 June 2017
Accepted 16 June 2017
Available online xxx

Keywords:
Drug-membrane interaction
Fluidity
Permeability
Langmuir
Cholesterol
Liposomes

ABSTRACT

Budesonide (BUD), a poorly soluble anti-inflammatory drug, is used to treat patients suffering from asthma and COPD (Chronic Obstructive Pulmonary Disease). Hydroxypropyl-β-cyclodextrin (HPβCD), a biocompatible cyclodextrin known to interact with cholesterol, is used as a drug-solubilizing agent in pharmaceutical formulations. Budesonide administered as an inclusion complex within HPβCD (BUD:HPβCD) required a quarter of the nominal dose of the suspension formulation and significantly reduced neutrophil induced inflammation in a COPD mouse model exceeding the effect of each molecule administered individually. This suggests the role of lipid domains enriched in cholesterol for inflammatory signaling activation.

In this context, we investigated the effect of BUD:HPβCD on the biophysical properties of membrane lipids. On cellular models (A549, lung epithelial cells), BUD:HPβCD extracted cholesterol similarly to HPβCD. On large unilamellar vesicles (LUVs), by using the fluorescent probes diphenylhexatriene (DPH) and calcein, we demonstrated an increase in membrane fluidity and permeability induced by BUD:HPβCD in vesicles containing cholesterol. On giant unilamellar vesicles (GUVs) and lipid monolayers, BUD:HPβCD induced the disruption of cholesterol-enriched raft-like liquid ordered domains as well as changes in lipid packing and lipid desorption from the cholesterol monolayers, respectively. Except for membrane fluidity, all these effects were enhanced when HPβCD was complexed with budesonide as compared with HPβCD. Since cholesterol-enriched domains have been linked to membrane signaling including pathways involved in inflammation processes, we hypothesized the effects of BUD:HPβCD could be partly mediated by changes in the biophysical properties of cholesterol-enriched domains.

1. Introduction

The concept of biological membranes has evolved from simple physical barriers providing individualization of the cell and subcellular compartments. This concept evolved to encompass cellular membrane complexity [1–5] regarding its (i) composition, including hundreds of lipid species, glycolipids and proteins; (ii) organization, including asymmetry and lateral domains; and (iii) function, *e.g.* signaling cascades, modulation of protein function and folding, cellular communication, pathogen and drug interaction, among many others.

The presence of non-random domains within the lipid bilayer, *e.g.* the so-called cholesterol and sphingolipid-enriched lipid rafts [6], further supports the functional character of the membrane over a simple structural role. Cholesterol and sphingomyelin (SM)-enriched domains show particular biophysical properties [7] creating an ordered (liquid ordered, l_o) lipid phase within the bulk membrane. Removal of cholesterol by a randomly methylated-β-cyclodextrin (MeβCD) from the lipid bilayer was shown to induce alterations in membrane biophysical properties [8]. Lipid rafts have been linked to several membrane functions including signaling activation by immune receptors such as TLR4 and CD44 [9] involved in inflammation and cancer [10]. Furthermore, changes in lipid membrane composition and/or biophysical properties leading to significant membrane reorganization have been linked to consequent disruption of cell signaling [11].

Cyclodextrins (CD) are cyclic oligosaccharides consisting of six (αCD), seven (βCD) or eight (γCD) glucopyranose units linked with

* Corresponding author at: FACM/LDRI-UCL - Cellular and Molecular Pharmacology Unit of the Louvain Drug Research Institute, Université catholique de Louvain, Avenue E. Mounier 73, B1.73.05. B-1200 Bruxelles, Belgium.
Email address: marie-paule.mingeot@uclouvain.be (M-P Mingeot-Leclercq)
[1] Both authors equally contributed to the study.

http://dx.doi.org/10.1016/j.bbamem.2017.06.010
0005-2736/

α-1,4 glycosidic linkages [12]. The toroidal shape and hydrophobic cavity of cyclodextrins allows the formation of inclusion complexes with hydrophobic molecules of adequate size and shape through non covalent interactions [13]. Hydroxypropyl-β-cyclodextrin (HPβCD) is an FDA/EMA approved β-cyclodextrin derivative with increased water solubility and low toxicity [14]. HPβCD is able to form complexes with surfactants [15] and polymers [16] as well as with drug molecules, such as curcumin [17] and budesonide [18].

Budesonide (BUD), a well-known anti-inflammatory drug is a glucocorticoid commercially available as Pulmicort®. Budesonide is recommended for the treatment of asthma [19,20], acute onset of Chronic Obstructive Pulmonary Disease (COPD) [21], allergic rhinitis [22] and Crohn's disease [23] among others, acting through the direct inhibition of expression of pro-inflammatory mediators [24]. Unfortunately, with a log*P* of 3.2, budesonide is practically insoluble in water at physiological pH, leading to low pulmonary deposition [25–27] and reduced bioavailability, requiring the use of relatively high doses in clinical use.

In patients with mild to moderate persistent asthma, budesonide administered as an inclusion complex within HPβCD (BUD:HPβCD) required a quarter of the nominal dose of the suspension formulation due to a marked reduction in nebulization time [25,28]. Moreover, co-administration of budesonide solubilized within HPβCD has been shown to significantly reduce neutrophil induced inflammation in a COPD mouse model exceeding the effect of each molecule administered individually (Rocks et al., unpublished data).

In this context, a clear understanding of the molecular mechanism of action of the BUD:HPβCD complex is essential to design tailored and optimized therapeutic formulations.

This work focused on studying the effect of the BUD:HPβCD complex on biophysical properties of lipid membrane. Since the BUD:HPβCD complex is envisaged for aerial administration by nebulization, lung epithelial cells (A549) are used for the study of its cellular toxicity and cholesterol extraction potential.

The effects of BUD:HPβCD on membrane biophysical properties were evaluated using membrane model systems. Large unilamellar vesicles (LUVs) were used to study the interaction with membrane cholesterol, via a fluorescent analogue of cholesterol (DHE), and changes in membrane fluidity and permeability, by using the fluorescent probes diphenylhexatriene (DPH) and calcein, respectively. Giant unilamellar vesicles (GUVs) were used to visualize the effect on lateral phase separation and lipid organization using fluorescence microscopy. Finally, Langmuir studies characterized the effect on lipid packing and desorption from the lipid monolayer.

2. Experimental procedures

2.1. Chemicals

The L-α-phosphatidylcholine (PC - Egg, Chicken), 1,2-dipalmitoyl-*sn*-glycero-3-phosphocholine (POPC), 1,2-dioleoyl-*sn*-glycero-3-phosphocholine (DOPC), egg sphingomyelin (SM - Egg, Chicken), *N*-palmitoyl-D-erythro-sphingosyl phosphoryl choline (pSM - 16:0 SM d18:1/16:0), L-α-phosphatidylinositol (PI - Liver, Bovine), cholesterol (Chol - ovine wool), ergosta-5,7,9(11),22-tetraen-3ß-ol (DHE - dehydroergosterol), 1,2-dioleoyl-*sn*-glycero-3-phosphoethanolamine-*N*-(lissamine rhodamine B sulfonyl) (ammonium salt) (18:1 Liss Rho-PE) and 1,2-dipalmitoyl-*sn*-glycero-3-phospho ethanolamine-*N*-(biotinyl) (sodium salt) (16:0 Biotinyl PE) were purchased from Avanti Polar Lipids (Alabaster, AL, USA). *N*-(7-Nitrobenz-2-Oxa-1,3-Diazol-4-yl)-1,2-Dihexadecanoyl-*sn*-Glycero-3-Phospho ethanolamine, Triethylammonium Salt) (NBD-PE) was purchased from Life Technologies (Leusden, Netherlands). 1,6-diphenyl-1,3,5-hexatriene (DPH), avidin from egg white, 16,17-Butylidenebis(oxy)-11,21-dihydroxypregna-1,4-diene-3,20-dione (Budesonide, BUD), Fluorescein-bis(methyliminodiacetic acid) (Calcein), and Sephadex® G-50 were purchased from Sigma-Aldrich (St. Louis, MO-USA). Methyl β-cyclodextrin (MeβCD, Crysmeb®) and Hydroxypropyl-β-cyclodextrin (HPβCD, Kleptose® Oral Grade) were purchased from Roquette (Lestrem, France).

Lipids and lipid probes were dissolved in chloroform, except DPH, which was dissolved in tetrahydrofuran (THF), and were kept at − 20 °C. The cyclodextrins were solubilized in PBS (NaCl 137 mM, KCl 2.7 mM, Na_2HPO_4 9.6 mM and KH_2PO_4 1.15 mM, pH 7.4) at their maximal concentration of 30 mM for MeβCD and 250 mM for HPβCD. Budesonide was firstly dissolved in DMSO at 100 mM and then diluted to 0.1 mM in a PBS solution (DMSO 0.1% v/v). All organic solvents used were Spectronorm grade from VWR (Radnor, PA, USA) or Emsure grade from Merck (Darmstadt, Germany).

2.2. Preparation of the Budesonide-Cyclodextrin complex

The Budesonide-Cyclodextrin complex (BUD:HPβCD) was prepared by adding budesonide to a HPβCD solution in PBS during 48 h under magnetic agitation or 2 h using a T-25 Ultra-Turrax® laboratory mixer from IKA (Staufen, Germany). The amount of budesonide effectively encapsulated was determined using HPLC-MS quantification as described by Dufour et al. [26].

2.3. A549 cell culturing, cytotoxicity assay and cholesterol dosage

A549 cells were cultured in DMEM medium – from Thermo-Fisher Scientific (Waltham, MA-USA) – supplemented with 10% of Fetal Bovine Serum (FBS) at 37 °C and under 5% CO_2. A549 cells, grown to 80% confluence in 96-well plates, were exposed to MeβCD, HPβCD, BUD:HPβCD complex and budesonide in low-serum conditions (1% FBS). Cell death was inferred from cell membrane permeabilization to cytoplasmic Lactate Dehydrogenase (LDH). LDH activity was measured in triplicate using the Cytotoxicity Detection Kit^{plus} (LDH) version 06 from Sigma-Aldrich (St. Louis, MO-USA).

The amount of protein was determined using the DC^{TM} Protein Assay Kit from Bio-Rad (Hercules, CA-USA).

After extraction, total cholesterol [29] was quantified using the Amplex® Red Cholesterol Assay Kit from Thermo-Fisher Scientific (Waltham, MA-USA).

2.4. Preparation of large unilamellar vesicles (LUVs)

Large unilamellar vesicles (LUVs) were prepared by extrusion from multilamellar vesicles (MLVs). Lipids were mixed at the molar ratios of PC:SM:PI (4:4:3) and PC:SM:PI:Chol (4:4:3:5.5) with a probe-to-lipid ratio of 1:100 for DHE and 1:300 for DPH and a final lipid concentration of 10 mM. A lipid film was obtained after solvent evaporation over 2 h, using a R-210 rotavapor from Buchi (Flawil, Switzerland) coupled to a vacuum pump HZ 2C from Vacuubrand (Wertheim, Germany), followed by minimum 2 h in an exsiccator under vacuum. The lipid film was hydrated in Tris-HCl buffer (Tris-HCl 10 mM, NaCl 135 mM, pH 7.4). MLVs were obtained by repeated cycles (× 7) of vortex/freeze/thawing. LUVs were obtained by MLV extrusion (× 21) using a mini-extruder system from Avanti Polar Lipids (Alabaster, AL, USA) with a 100 nm pore size polycar-

bonate Nuclepore Track Etch membrane filter from Whatman® (GE Healthcare, Little Chalfont, UK). Total lipids were quantified using the method from Rouser [30] and diluted to the desired final concentration in PBS.

2.5. Vesicle size and ζ-potential determinations

LUV mean size and ζ-potential were determined using a Zetasizer Nano SZ equipment from Malvern Instruments (Grovewood Road, UK) with patented NIBS (non-invasive back scatter) technology and the recommended software. Particle size distribution and the polydispersion index (PdI) measurements were performed by Dynamic Light Scattering (DLS) technology using 12 mm square polystyrene cuvettes in a thermostated chamber at 25 °C. Particle charge (ζ-potential) was measured using Dynamic Electrophoretic Mobility (DEM) using a disposable folded capillary cell in a thermostated chamber at 25 °C.

2.6. Fluorescence spectroscopy measurements

All fluorescence measurements were carried out with a LS55 spectrofluorimeter from Perkin Elmer (Waltham, MA-USA) in right angle geometry. Temperature was stabilized at 25 °C using a C25P Phoenix II thermostating water bath from Thermo Scientific (Waltham, MA-USA).

2.7. Dehydroergosterol (DHE) Spectroscopy

The ability of BUD:HPβCD and HPβCD to bind to cholesterol was investigated using DHE fluorescence spectroscopy.

DHE (10 μM) was prepared in PBS pH 7.4 containing 0.1% DMSO [31]. Fluorescence emission spectra of DHE in buffer solution were recorded at increasing concentrations of BUD:HPβCD or HPβCD, and the intensity of the monomeric versus microcrystalline peak ratio was plotted against log10 concentration. The excitation monochromator was set at 328 nm, and the emission spectra were recorded from 340 to 545 nm [32,33]. The influence of DMSO and DHE concentration was controlled.

To probe the interaction between BUD:HPβCD or HPβCD with cholesterol in a lipid environment, 1 mol% of DHE was incorporated in LUVs composed of PC:SM:PI:Chol (4:4:3:5.5). Maximal emission of DHE was observed around 372, 404 and 424 nm, as described previously in membrane systems [34]. LUVs (5 μM) were incubated with increasing BUD:HPβCD or HPβCD concentrations for 3 h at 25 °C.

2.8. Diphenylhexatriene fluorescence polarization

Molecule polarization was quantified using steady state fluorescence anisotropy, $< r >$, measurements calculated using Eq. (1):

$$\langle r \rangle = \frac{I_{VV} - GI_{VH}}{I_{VV} + 2GI_{VH}} \quad (1)$$

where the different intensities I_{IJ} are the steady state polarized vertical and horizontal components of fluorescence emission with excitation vertical (I_{VV} and I_{VH}) and horizontal (I_{HV} and I_{HH}) to the emission axis. The latter pair of components was used to calculate the G factor ($G = I_{HV} / I_{HH}$).

DPH concentration was determined by UV spectroscopy and adjusted to 100 μM in tetrahydrofuran. Final lipid concentration was adjusted to 50 μM in PBS pH 7.4. LUVs were incubated with BUD:HPβCD or HPβCD for 60 min at 25 °C shielded from light.

2.9. Calcein release

Changes in the membrane permeability were followed by determining the leakage of entrapped calcein at self-quenching concentrations, from liposomes [35]. Briefly, the dried lipid films were hydrated with a solution of purified calcein (73 mM) in Tris-HCl buffer at pH 7.4 and osmolarity of 404 mOsm/kg. The un-encapsulated dye was removed by the mini-column centrifugation technique using Sephadex® G-50 [36]. The liposomes were diluted to a final lipid concentration of 5 μM in an isosmotic Tris-HCl (Tris 10 mM and NaCl 188 mM) pH 7.4 buffer and stabilized for 10 min at 25 °C. Values were recorded for 30 s before addition of BUD:HPβCD or HPβCD at increasing final concentrations of 10 and 20 mM. After the addition of the compounds, the fluorescence intensities were continuously recorded as a function of time for up to 500 s. The percentage of calcein released was determined according to Eq. (2):

$$\left[\left(F_t - F_{contr}\right) / \left(F_{tot} - F_{contr}\right)\right] \times 100 \quad (2)$$

where F_t is the fluorescence signal measured at a time t in the presence of compounds, F_{contr} is the fluorescence signal measured at the same time t for control liposomes, and F_{tot} is the total fluorescence signal obtained after complete disruption of the liposomes by 0.02% Triton X-100.

2.10. Preparation of giant unilamellar vesicles (GUVs)

Giant unilamellar vesicles (GUVs) were prepared using the electroformation method [37–39]. In brief, mixtures of DOPC:pSM (1:1) and DOPC:pSM:Chol (1:1:3) with biotinylated lipid-to-lipid ratio of $1{:}10^6$ Biotinyl-PE and probe-to-lipid ratio of 1:750 for Rho-DOPE and 1:250 for NBD-PE were prepared. A small volume (4 μl) of lipid mixture (4 mM) was evenly spread on the surface of an ITO coated glass lamella and the solvent was allowed to evaporate over 5 min. A 1 mm thick silicon gasket was used to form a sealed reaction chamber. Sucrose-Tris (475 μL) was added and a second ITO covered glass lamella was overlaid. The GUVs were formed at 60 °C over a 2 h exposure to a sinusoidal signal with a peak-to-peak intensity of 1 V and frequency of 500 Hz. The GUVs were used within the day.

2.11. Fluorescence microscopy measurements

GUVs were used to visualize the lipid lateral segregation and phase separation. GUVs were placed in a μ-Slide 8-well chamber from Ibidi (Martinsried, Germany) previously coated with avidin 0.1% for a minimum of 2 h. GUVs were observed using an Axio Observer Z1 inverted microscope (Carl Zeiss, Jena, Germany) equipped with a model CSU-X1 spinning disk (Yokogawa Electric Corporation, Tokyo, Japan) and a Plan-Apochromat 100 ×/1.40 Oil DIC M27 objective (Carl Zeiss, Jena, Germany). Images were recorded and analyzed with an AxioCamMR3 camera using Carl Zeiss AxioVision® 4.8.2 software. The red channel was used for Rho-DOPE (excitation/emission at 561/617 nm) and in the green channel for NBD-PE (excitation/emission at 488/530 nm).

2.12. Surface pressure–area (π-A) compression isotherms

To examine the effect of BUD:HPβCD and HPβCD, on lipid packing, surface pressure–area (π-A), compression isotherms were recorded with an automated Langmuir trough (KSV Mini-trough KSV Instruments Ltd., Helsinki, Finland-width = 7.5 cm, length = 37 cm), two hydrophilic Delrin mobile barriers (symmetric compression), a platinum Wilhelmy plate, and a temperature probe. The system was enclosed in a Plexiglas® box, and the temperature was maintained at 22.0 ± 1.0 °C.

The cleanliness of the surface was ensured by aspiration of the sub-phase surface before each experiment. Once the temperature was stabilized, the barriers were fully closed and reopened and, if a variation in surface pressure of less than 0.5 mM/m was observed, the lipid was deposed on the air-liquid interface surface with a micro-syringe (Hamilton, USA). The platinum plate was cleaned by rinsing with isopropanol and heating to red glow in-between experiments. PBS pH 7.4 was used as the subphase. Lipids (Chol, SM, POPC, or the negatively-charged lipid, PI) were dissolved at a concentration of 2 mM in $CHCl_3$:MeOH (2:1 v/v) and were spread at the liquid/air interface with a micro-syringe (Hamilton, USA). The volume was chosen in order to obtain an optimal isotherm compression curve (starting at 0 mN/m and showing a collapse at the end of the compression).

After an equilibration time of 15 min, the film was compressed at a rate of 10 mm/min. BUD:HPβCD (0.04:1 mM:mM) or HPβCD (1 mM) were solubilized in the subphase before spreading the lipid using the same amount of lipid as for the control assays. The same procedure as the one used for experiments without cyclodextrin was applied. Each compression isotherm was repeated at least two times; the relative standard deviation in surface pressure and area was ≤ 5%.

2.13. Surface pressure–time (π-t) adsorption isotherms

BUD:HPβCD or HPβCD effect on lipid molecular area were assessed by measuring lipid molecular area over time upon incubation with the compounds (π-t isotherms). To this end, the same set-up as described for the surface pressure–area (π-A) compression isotherms was used with a different automated Langmuir trough (KSV Mini-trough KSV Instruments Ltd., Helsinki, Finland-width = 7.5 cm, length = 20 cm).

The lipids (Chol, SM, POPC, or PI) were added until a surface pressure of 30 mN/m was achieved and, after a stabilization period of 15 min, surface pressure over time was recorded. After the acquisition of a 200 s baseline to verify the stability of the monolayer, the compounds were injected into the subphase using specialized injection supports to a final concentration of 0.04:1 mM:mM of BUD:HPβCD or 1 mM of HPβCD. Surface pressure was recorded until a plateau was observed.

The obtained curves were analyzed by a fitting on a 2-phase exponential regression from where the estimated plateau values were extracted.

2.14. Statistical analysis

All data manipulation, graphical presentation and statistical analysis was performed using Microsoft® Excel® (2016, Microsoft®, Redmond – Washington USA) and GraphPad Prism® (version 4.03 for Windows, GraphPad Software Inc., La Jolla - California USA, www.graphpad.com).

3. Results

3.1. Cell toxicity and cell cholesterol depletion

We first evaluated the cytotoxicity of the complex BUD:HPβCD in comparison with the highly hydrophobic anti-inflammatory drug, budesonide (BUD) and HPβCD.

The cytotoxic effect was determined by following LDH release on lung epithelial cells (A549). For concentrations in cyclodextrin varying from 0 to 10 mM and after 4 h of incubation (Fig. 1.a), the cytotoxicity induced by BUD:HPβCD or HPβCD was lower (*ca.* 10%) as compared with budesonide. At 25 mM in cyclodextrin and

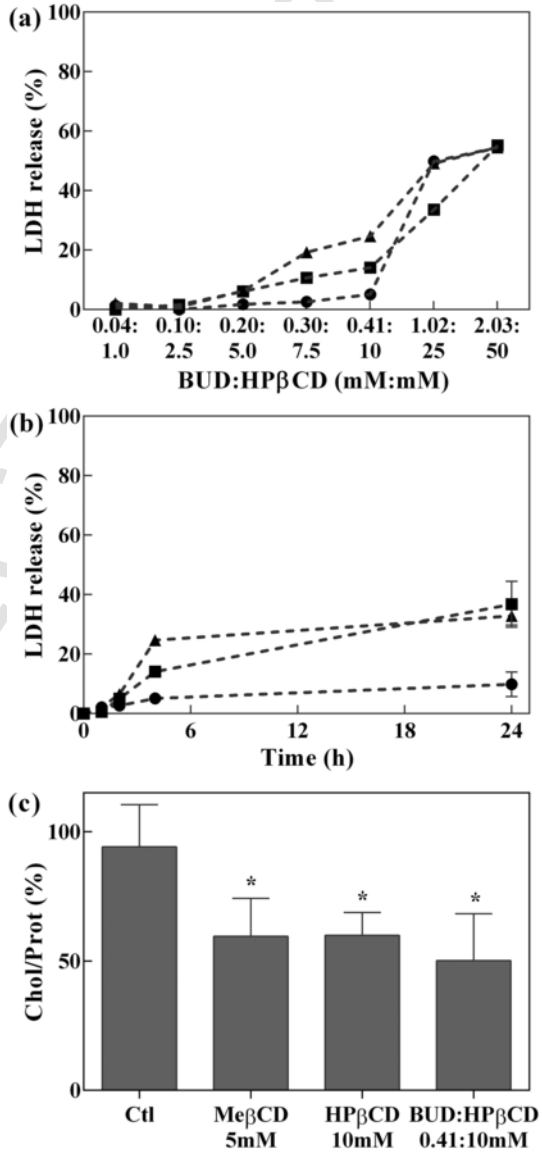

Fig. 1. Cell toxicity and effect on cholesterol of BUD:HPβCD, HPβCD, and BUD on lung epithelial cells. Percentage of LDH released from A549 lung epithelial cells (a) at 4 h for BUD:HPβCD (squares) 0.04:1 to 2.03:50 mM:mM, HPβCD (circles) 1 to 50 mM in cyclodextrin, or BUD (triangles) 0.04 to 2.03 mM and (b) for BUD:HPβCD 0.41:10 mM:mM (squares), HPβCD 10 mM (circles), or BUD 0.41 mM (triangles) at 1, 2, 4 and 24 h. (c) Total cellular cholesterol (normalized to total amount of proteins) for A549 lung epithelial cells treated with BUD:HPβCD 0.41:10 mM:mM, HPβCD 10 mM, or MeβCD 5 mM, for 45 min normalized to untreated A549 cells.

over, significant toxicity (*ca*. 40%) was observed. Regardless the concentrations in cyclodextrin (from 0 to 25 mM), the cytotoxicity induced by the complex (BUD:HPβCD) was lower as compared to that observed with budesonide alone. At 50 mM in cyclodextrin, cytotoxicity was comparable for HPβCD, BUD:HPβCD and budesonide. Regarding the time dependency cytotoxic effect induced by BUD:HPβCD (0.41:10 mM:mM), budesonide (0.41 mM), and HPβCD (10 mM) (Fig. 1.b), we didn't have any effect for 2 h of incubation. After 4 h, LDH release started and after 24 h of incubation, BUD:HPβCD and budesonide, showed more than 35% of LDH release. In comparison, HPβCD induced less than 10% LDH release.

Selecting non-toxic conditions, we quantified the extraction of cholesterol from cells (Fig. 1.c). MeβCD (5 mM) was used as a positive control. For BUD:HPβCD (0.41:10 mM:mM) and HPβCD (10 mM), after 45 min of incubation, the amount of total cholesterol (normalized to total protein) was reduced by *ca*. 45%. HPβCD was able to significantly extract cholesterol from the membrane regardless of previous complexation with budesonide.

3.2. Interaction with membrane model systems

The effect of the extraction of cholesterol induced by BUD:HPβCD and HPβCD on membrane biophysical properties was further characterized in membrane model systems.

To determine the concentration range of HPβCD without vesicle destabilization, vesicle mean size and ζ-potential were measured upon incubation with increasing concentration of HPβCD (up to 100 mM, Fig. S1). Briefly, at ratios of HPβCD:lipid exceeding 5000:1 (HPβCD 25 mM to lipids 5 μM), the fraction of vesicles within the diameter range of the control samples became significantly reduced. Therefore, a 25 mM threshold of HPβCD was set to avoid experimental artefacts and/or skewed results.

3.3. Interaction with sterols in aqueous solution

The interaction of BUD:HPβCD and HPβCD with cholesterol was studied using a cholesterol analogue presenting similar behavior in aqueous solution and biological membranes [33,34,40], the dehydroergosterol (DHE). Especially, it shows similar properties regarding lateral phase separation compared to cholesterol [41]. Lateral interactions between sterols are responsible for an increase in DHE fluorescence quantum yield at higher wavelengths of emission [32,42,43]. DHE is a self-quenching molecule and fluorescence emission of the monomeric peak (I_{372}) occurs upon the dissolution of cholesterol-enriched domains [44] or desorption of DHE from the lipid bilayer [45] by βCDs. DHE aggregates in solution can be quantified using the fluorescence emission ratio I_{372}/I_{424} [34], corresponding to the monomeric species over the aggregate forms, such as DHE microcrystals in solution [34,42]. The spectral properties of DHE, namely fluorescence intensity and peak ratios (I_{372}/I_{424}), are used to infer upon the microenvironment of cholesterol, in agreement with results showing comparable, although slightly faster, extraction of DHE in mixed monolayers (sterols:POPC 30:70) by HPβCD, to that of cholesterol [45].

The interaction of increasing concentrations of BUD:HPβCD and HPβCD with DHE in solution was characterized (Fig. 2) and comparative control studies were performed using MeβCD (Fig. S2, a, b). An increase of the intensity of the monomeric peak at 372 nm (Fig. 2.a), concomitant with an increase in the ratio of the monomeric over the aggregate form of DHE (Fig. 2.b) was observed. The effect started at 1 mM HPβCD and a plateau value was reached at 10 mM. Regarding the ratio of the monomeric over the aggregate form of DHE (I_{372}/I_{424}), the effect was observed at slightly lower concentrations of HPβCD when complexed with the budesonide. No effect was observed for budesonide alone (not shown). Overall, the increase in fluorescence of the DHE monomeric peak indicates the solubilisation of DHE by the HPβCDs in a concentration dependent manner, which is likely due to the formation of HPβCD-sterol complexes as previously described [45].

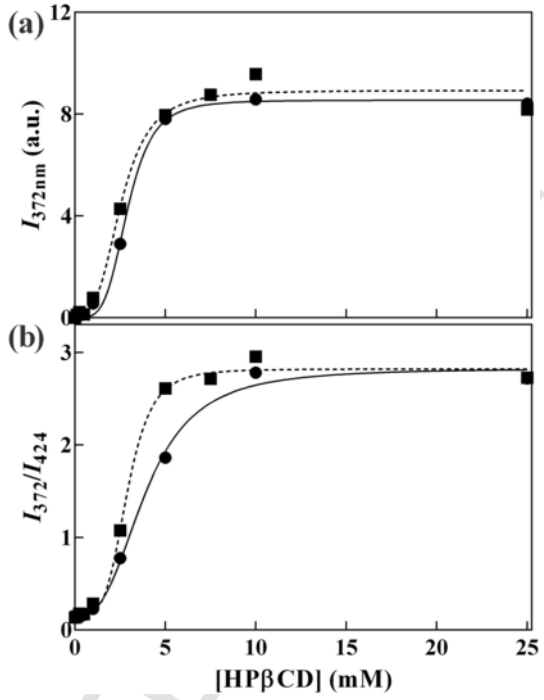

Fig. 2. Fluorescence of DHE in aqueous solution upon interaction with BUD-HPβCD, and HPβCD. (a) Fluorescence emission intensity at 372 nm and (b) ratio of peak intensity between 372 and 424 nm upon addition of BUD:HPβCD (squares; dotted line), or HPβCD (circles; solid line). The lines correspond to a non-linear fitting of a non-logarithmic sigmoidal Hill growth function to the data.

3.4. Interaction with sterols in a lipid membrane

In order to study the effect of increasing concentrations of cyclodextrin (HPβCD and BUD:HPβCD) on the microenvironment of cholesterol within lipid bilayers, a small fraction of DHE was incorporated into LUVs mimicking the lipid composition of plasma membrane (PC:SM:PI:Chol 4:4:3:5.5) (Fig. 3) and comparative control studies were performed using MeβCD (Fig. S2, c, d).

Fig. 3 presents the fluorescence intensity at the 372 nm emission peak of DHE monomeric form (Fig. 3.a) and the ratio of emission at 372 nm over 424 nm (Fig. 3.b) upon interaction with the BUD-HPβCD complex and HPβCD. An increase in fluorescence intensity of DHE (Fig. 3.a) was observed, which was less pronounced as compared with DHE microcrystals in solution. This can be due to the lower amount of DHE within the membranes (200 × less concentrated). Moreover, DHE microenvironment can affect βCD potential for complexing with cholesterol [45], the dissolution of an aggregate form in solution being likely facilitated over the extraction of DHE stabilized within a lipid membrane. The results showed that, regardless of complexation with budesonide, HPβCD was able to increase the fluorescence of DHE monomeric peak. Regarding the ratio of the monomeric over the aggregate form of DHE within the bilayer (Fig. 3.b), it was comparable to that of DHE microcrystals solubilized

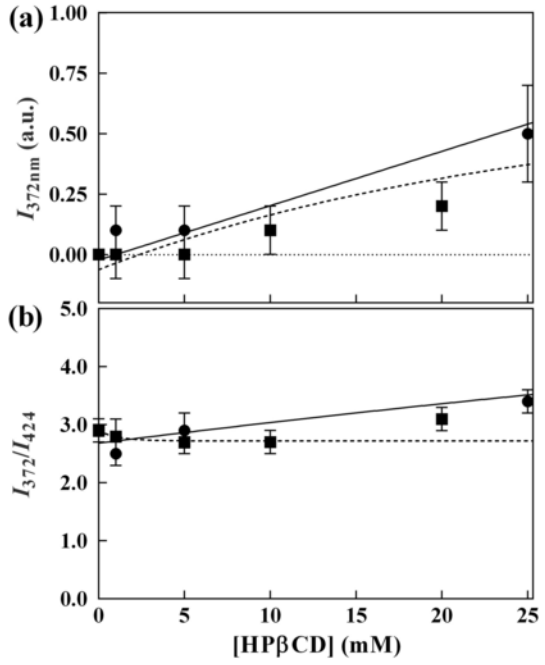

Fig. 3. Fluorescence of DHE within LUVs upon interaction with BUD:HPβCD, and HPβCD. (a) Emission at the monomeric 372 nm peak and (b) ratio of emission at 372 nm over 424 nm upon interaction with BUD-HPβCD (squares; dotted line), or HPβCD (circles; solid line), with LUVs composed of PC:SM:PI:Chol 4:4:3:5.5. DHE was present at 1 mol% of total lipid concentration. Measurements were performed at 25 °C in triplicate. The lines correspond to a non-linear fitting of a non-logarithmic sigmoidal Hill growth function to the data.

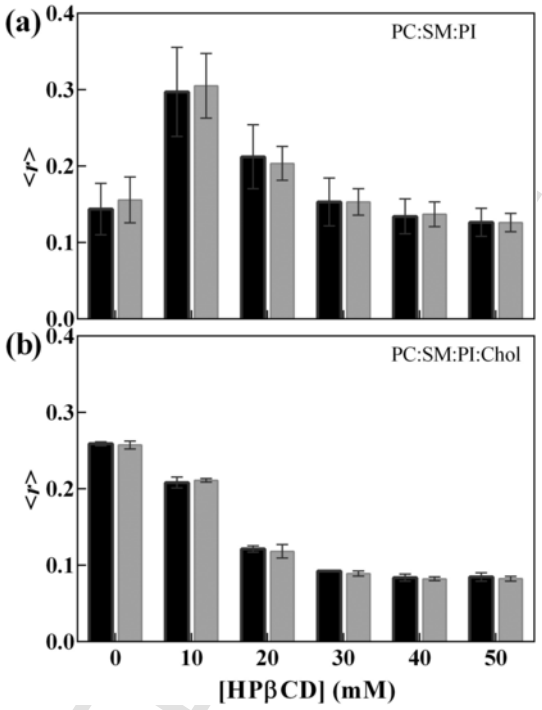

Fig. 4. Membrane fluidity measurements of LUVs containing and lacking cholesterol upon interaction with BUD:HPβCD, and HPβCD. Measurement of DPH anisotropy (< *r* >) upon addition of BUD:HPβCD complex (grey bars), or HPβCD (black bars) to LUVs composed of (a) PC:SM:PI (4:4:3) or (b) PC:SM:PI:Chol (4:4:3:5.5) containing DPH (1:300 molar ratio).

by the HPβCD (Fig. 2.b). No major difference was observed when the effect of BUD-HPβCD was compared to that of HPβCD.

DHE de-quenching can be due to either the disruption of cholesterol-enriched domains [34] or to extraction from membrane by the HPβCD [45]. Measurements of emission intensity over time (data not shown) showing an instantaneous endpoint de-quenching of DHE, suggest DHE extraction from the membrane instead of the rearrangement of lipid lateral organization, which would occur over several minutes. Overall, increase in DHE monomeric peak emission by BUD:HPβCD or HPβCD demonstrated changes of the sterol environment in agreement with DHE extraction from the membrane [44]. Because cholesterol is a main modulator of membrane fluidity, its extraction from membrane by BUD:HPβCD and HPβCD could modify membrane fluidity.

3.5. Effect on membrane fluidity

Cholesterol increases the fluidity of very ordered domains and increases the rigidity of very disordered domains. Moreover, cholesterol and sphingolipid-enriched domains, *i.e.* raft-like domains, present decreased fluidity and hydration when compared to the bulk membrane.

The lipid dynamics of acyl lipid chains can be monitored using diphenylhexatriene (DPH), a dye that probes the hydrophobic core of the membrane [46]. The degree of polarization of DPH, measured by its fluorescence anisotropy (< *r* >), increases as membrane fluidity decreases. Fig. 4 shows the variation of DPH anisotropy in LUVs lacking cholesterol (PC:SM:PI 4:4:3) and LUVs containing cholesterol (PC:SM:PI:Chol 4:4:3:5.5) upon interaction with the BUD:HPβCD complex or HPβCD.

For vesicles lacking cholesterol, the results (Fig. 4.a) show a fluid membrane (l_d) in the absence of cholesterol (< *r* > of *ca*. 0.15), as is expected for a lipid mixture containing phospholipid:sphingolipid at a molar ratio of 7:4 at 25 °C [47]. Adding cholesterol (Fig. 4.b) reduced membrane fluidity (< *r* > of *ca*. 0.25), indicating the presence of a liquid ordered (l_o) phase typical of a mixture containing *ca.* 33 mol% of cholesterol and 25 mol% of SM at 25 °C [47].

Upon incubation of cholesterol-free vesicles with HPβCD (Fig. 4.a), an increase in DPH anisotropy to values suggesting a gel phase (< *r* > of *ca*. 0.30) was observed at the lower concentration of HPβCD (10 mM). Increasing HPβCD concentration caused a concentration dependent increase in membrane fluidity back to control values. These results are in agreement with literature [48,49,50]. Since we excluded increase in average size of liposomes (Fig. S1) as suggested in literature [48,49], the formation of supra-molecular cyclodextrin structures on the surface of the lipid bilayer is likely the mechanism involved in decrease in membrane fluidity [50].

The incubation of BUD:HPβCD complex or HPβCD with cholesterol-enriched membranes (Fig. 4.b) resulted in a dose-dependent decrease of anisotropy indicating an increase in membrane fluidity. This effect reached a plateau at a value of anisotropy indicative of a very fluid cholesterol-free membrane (< *r* > of *ca*. 0.10) at 30 mM of CD. Moreover, the cholesterol depleted membrane by HPβCD became more fluid (< *r* > of *ca.* 0.10) than the control mixture without cholesterol (< *r* > of *ca*. 0.15). As for the cholesterol-free LUVs, the extraction of other membrane rigidifying lipids, such as the high T_m sphingolipid, sphingomyelin also located within the lipid raft, is likely. Despite a larger affinity of βCD towards cholesterol, other lipids may also be extracted from the membrane with varying affinities [45].

As was observed for DHE extraction from the membrane, HPβCD complexation with budesonide did not show any effect on the induced changes to membrane fluidity as compared with HPβCD. The presence of free budesonide did not change the membrane fluidity.

In conclusion, BUD:HPβCD or HPβCD incubation with cholesterol-enriched membranes lead to increased membrane fluidity. This is in agreement with the extraction of cholesterol and destabilization of the liquid ordered cholesterol- and sphingolipid-enriched raft-like domains. Altogether, this suggests a lateral reorganization of the lipids, which could be associated with increased membrane permeability.

3.6. Effect on membrane permeability

Permeation of the plasma membrane is often the first barrier for drug entry into the cell, as is the case for budesonide. Therefore, increased membrane permeability may be one of the possible modulators of drug bioavailability and efficacy. The permeabilization of the membrane can be determined by quantifying the increase in fluorescence emission of the self-quenching calcein upon release from permeabilized membranes. Calcein fluorescence intensity was measured upon interaction of BUD-HPβCD (0.41:10 mM:mM and 0.82:20 mM:mM) or HPβCD (10 and 20 mM) with vesicles lacking cholesterol (PC:SM:PI 4:4:3) and vesicles containing cholesterol (PC:SM:PI:Chol 4:4:3:5.5) (Fig. 5 and Fig. S3).

In the absence of cholesterol, BUD:HPβCD (20 mM in cyclodextrins) did not induce calcein leakage. In the presence of cholesterol, the extent of permeabilization increased to reach a plateau value (around 30% of calcein release) after 200 s (Fig. 5.top). The effect was dependent upon the concentration of cyclodextrins (10 mM < 20 mM in cyclodextrins) (Fig. 5.middle). These results were consistent with the increase in lipid extraction and consequent leakage of encapsulated calcein.

As compared to HPβCD alone, incubation with the BUD:HPβCD increased the rate of calcein release (Fig. 5.bottom) without affecting the percentage of calcein released at equilibrium. The increase in rate of membrane permeabilization may be explained by either (i) permeation of budesonide through the membrane or (ii) increase in HPβCD affinity towards the membrane induced by budesonide.

3.7. Effect on membrane phase separation

The interaction of BUD:HPβCD and HPβCD with cholesterol may lead to the disruption of the lipid raft domains, typically composed of cholesterol and sphingolipids.

Confocal fluorescence microscopy was used to observe the changes in lipid phase separation over time upon interaction with BUD:HPβCD or HPβCD. Control GUVs and lipid-raft model GUVs, composed of DOPC:pSM (1:1) and DOPC:pSM:Chol (1:1:3) [50], were labeled with Rho-DOPE (red channel) and NBD-PE (green channel) for the liquid disordered (l_d) and liquid ordered (l_o) domains, respectively.

Typically, the GUV population was relatively heterogeneous regarding vesicle size with diameters centered on *ca*. 15 μm (± 5 μm). Overall, no effect was observed by incubation with budesonide.

While the majority of the GUVs immediately presented changes in lipid phase separation upon interaction with the HPβCD, a subpopulation, mostly comprised of the very small GUVS (under 10 μm in diameter) began to exhibit observable changes only after more than 30 min of incubation or remained apparently unaffected.

In the absence of cholesterol (Fig. 6-left), the DOPC:pSM 1:1 membranes show a l_d/s_o (red/dark) phase separation as expected [47].

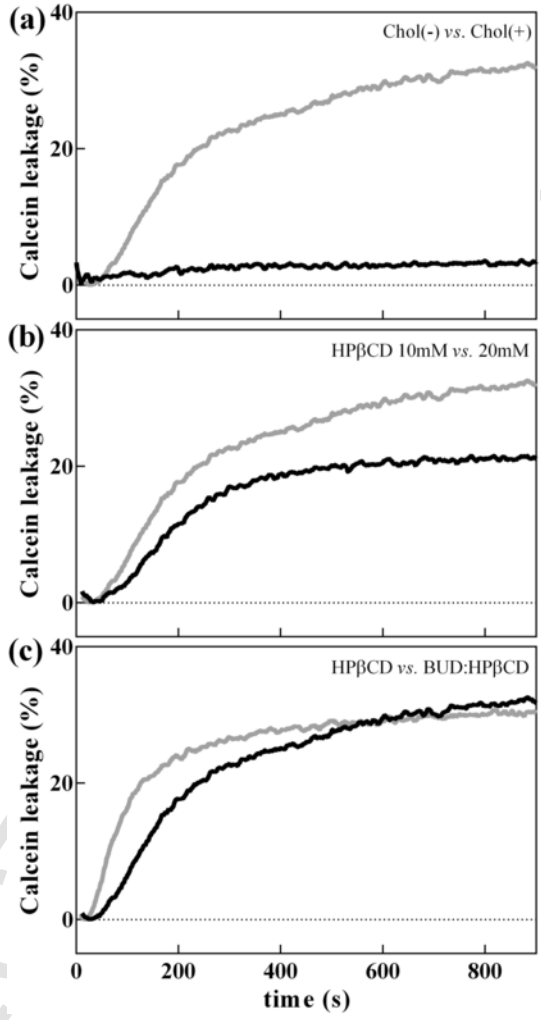

Fig. 5. Calcein leakage from LUVs containing and lacking cholesterol upon interaction with BUD:HPβCD, and HPβCD. Comparison of leakage of calcein (top) from PC:SM:PI (black line) and PC:SM:PI:Chol (gray line) vesicles in the presence of BUD:HPβCD 0.82:20 mM:mM; (middle) from PC:SM:PI:Chol vesicles in the presence of BUD:HPβCD 0.41:10 mM:mM (black line) and BUD:HPβCD 0.82:20 mM:mM (gray line); and (bottom) from PC:SM:PI:Chol vesicles upon interaction with BUD:HPβCD 0.82:20 mM:mM (gray line) and 20 mM of HPβCD 20 mM (black line). The curves are representative of three independent experiments.

Interaction with either BUD:HPβCD or HPβCD removed any microscopic phase separation and a single l_d phase (red) was observed. As was observed for the kinetics of membrane permeabilization (Fig. 5.c), the effect occurred at earlier incubation times for the BUD:HPβCD (under 5 min) when compared with the HPβCD alone (*ca*. 15 min).

In the presence of cholesterol (Fig. 6-right), no microscopic l_d/l_o phase separation was visible as expected for a mixture containing 60 mol% of cholesterol. Interaction with the HPβCD, and BUD:HPβCD alike, caused the appearance of observable l_o domains after 5 min of incubation, congruent with a decrease in the molar fraction of cholesterol. Longer incubation times showed further decrease of the l_o phase giving yield to l_d domains (eventually a single l_d phase was visible). Within 45 min, a l_d/s_o phase separation was observed, indicating a negligible amount or the absence of cholesterol within the membrane.

The decrease and, ultimately, the disappearance, of the liquid ordered phase (l_o), a phase enriched in cholesterol and sphingomyelin,

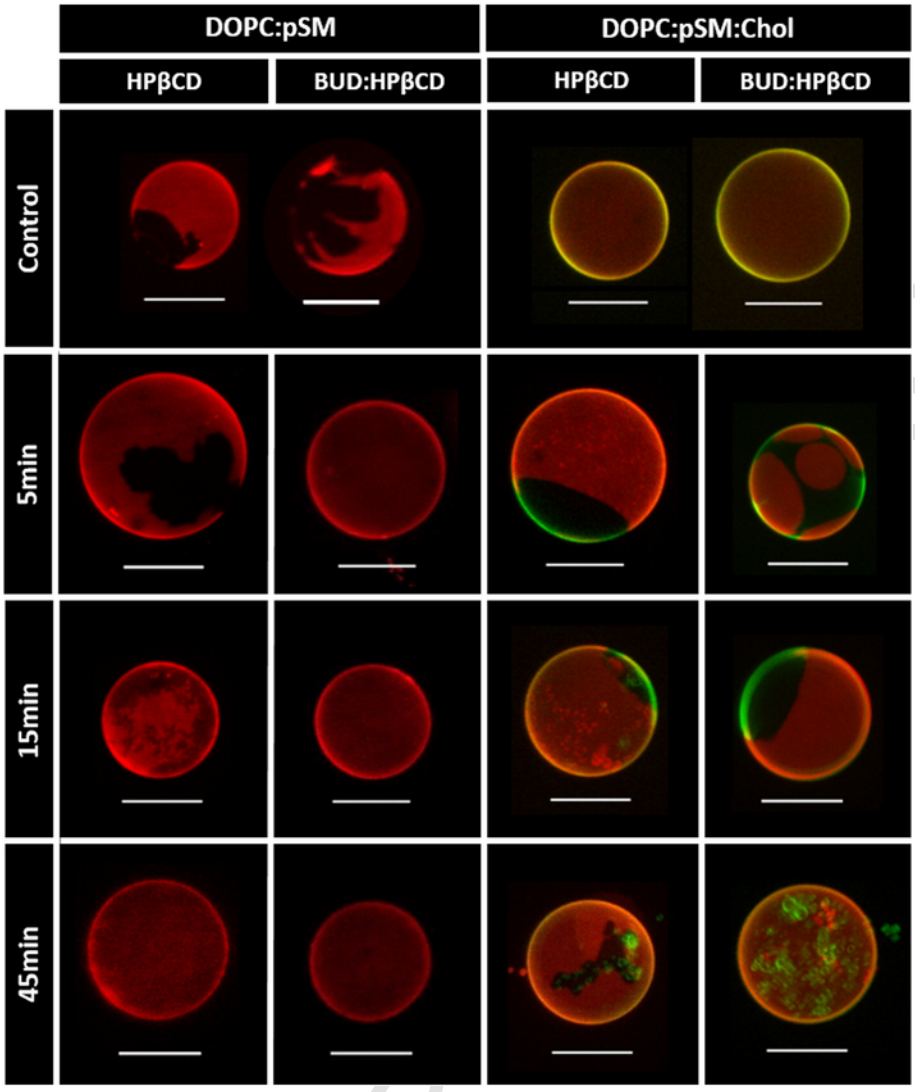

Fig. 6. Confocal fluorescence microscopy imaging of membrane phase separation in GUVs upon incubation with BUD:HPβCD, and HPβCD. Imaging of membrane domains in GUVs composed of (left) DOPC:pSM (1:1) and (right) DOPC:pSM:Chol (1:1:3) before (top, control) and after (descending) 5, 15 and 45 min with the BUD:HPβCD complex or HPβCD. DOPC:pSM vesicles were labeled with Rho-DOPE (red channel) to visualize the liquid disordered (l_d)/solid ordered (s_o) phase separation in red/dark. DOPC:pSM:Chol were labeled with Rho-DOPE (red channel) and NBD-PE (green channel) to visualize the liquid disordered (l_d)/liquid ordered (l_o) phase separation in red/green channels, respectively. The absence of fluorescent labelling indicates a solid ordered phase (s_o) and the co-localization of both probes (yellow) indicates a lack of observable phase separation.

is consistent with removal of cholesterol from the membrane by interaction with HPβCD [51].

3.8. Effect on lipid mean molecular area

To further characterize the effect of BUD:HPβCD and HPβCD on the biophysical membrane properties, we compared the isotherms of lipid monolayers spread with BUD:HPβCD or HPβCD aqueous solutions to those deposited on PBS buffer (Fig. 7).

In presence of BUD:HPβCD or HPβCD, a long plateau at a non-zero surface pressure was observed at large molecular areas whatever the composition of the monolayer. It suggests that BUD:HPβCD or HPβCD are able to adsorb to the lipid monolayer in a gaseous state [52,53] despite the fact that they do not change the surface pressure by themselves in the absence of lipids.

For all the lipids, further compression of monolayers in presence of BUD:HPβCD and HPβCD induced a progressive increase of the surface pressure indicating the formation of a liquid-expanded monolayer. Finally, at low molecular areas, the isotherms showed either a final plateau at constant surface pressure or a sharp decrease in surface pressure corresponding to the collapse of the monolayer. In the case of cholesterol (Fig. 7.a) and SM (Fig. 7.b) monolayers and in a lesser extent for PI (Fig. 7.d) monolayers, the profile of the lipid isotherm in the presence of BUD:HPβCD or HPβCD is different from that expected if the lipid molecules were simply removed from the interface. The lipid/ BUD:HPβCD or HPβCD interactions leads to the formation of new system at the interface.

The molecular area and surface pressure at which the membrane collapsed (referred to as A_C and SP_C, respectively) were used to quantitatively compare the interfacial behavior of lipids in presence or in absence of BUD:HPβCD or HPβCD (Fig. 7.e and f).

In the case of cholesterol monolayers (Fig. 7.a and e), a decrease in A_C (Fig. 7.a and e) was observed with BUD:HPβCD to a higher extent as compared with HPβCD. A reduction of the lipid molecular area in presence of exogenous drug can arise from desorption of the interfacial material into the subphase and/or from a reorganization of

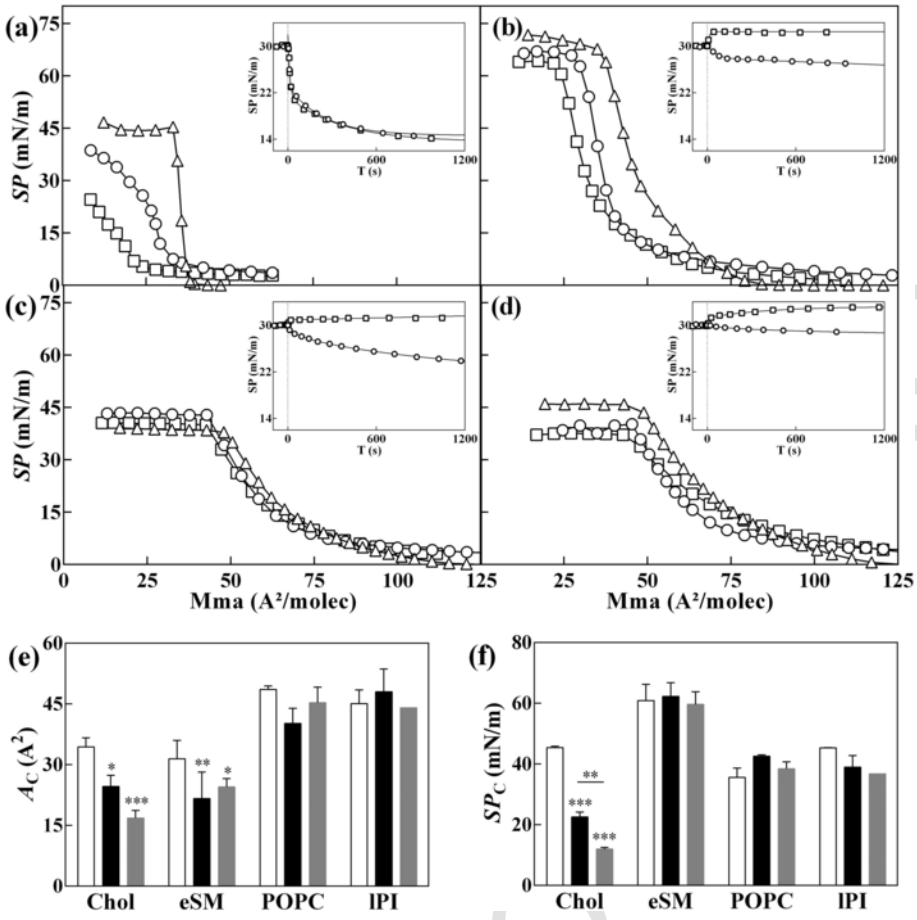

Fig. 7. Effect of BUD:HPβCD, and HPβCD on Chol, eSM, POPC and PI monolayers. Surface pressure-area (*Π-A*) compression isotherms of the pure lipids (a) Chol, (b) eSM, (c) POPC and (d) PI with a subphase composed of PBS (triangles), BUD:HPβCD 0.2:5 mM:mM (squares), or HPβCD 5 mM (circles). (inset) Surface pressure-time (*Π-t*) curves for the lipids with a subphase composed of PBS with BUD:HPβCD 0.04:1 mM (squares), or HPβCD 1 mM (circles) fitted with a non-linear regression curve. (e) Molecular area at the surface pressure onset (A_0) and (f) two-dimensional compressibility factor (C_s) for the higher compression for the pure lipid (light grey) and in the presence of BUD:HPβCD (dark grey) or HPβCD (grey) calculated from the surface pressure-area (*Π-A*) isotherms as described by [61]. The curves were recorded at 22 °C (± 1 °C) and are representative of replicated assays.

the interfacial monolayer (domain packing, nucleation) [53]. The significant decrease in SP_C (Fig. 7.f) in presence of HPβCD and even much more in presence of BUD:HPβCD means that the interaction of HPβCD destabilizes the liquid-condensed phase of the cholesterol monolayer, which is in accordance with the fluidification effect shown by DPH fluorescence polarization.

The injection of BUD:HPβCD or HPβCD beneath the cholesterol monolayer initially spread at the air-water interface until a surface pressure of 30 mN/m and maintained at a constant spreading surface gave rise to a rapid and important decrease of the surface pressure (Fig. 7.a-inset). These results are in favor of cholesterol depletion from the interface, as also shown for βCD in previous studies [45,52,53].

HPβCD and BUD:HPβCD also reduces the A_C of SM monolayers (Fig. 7.b and e) without significantly affecting SP_C (Fig. 7.f) suggesting some lipid desorption from the interface without changing lipid packing. The extraction of SM from the interface by HPβCD was in agreement with the decrease of surface pressure in the time-dependence surface pressure experiments. In contrast, BUD:HPβCD increased the surface pressure when it is injected under the SM monolayer. This suggests that two parallel phenomena occurs when BUD:HPβCD interacts with the SM monolayer, (i) a limited depletion of SM from the monolayer and (ii) an adsorption of BUD:HPβCD molecules to the interface.

In the case of POPC monolayers (Fig. 7.c, d, e), the presence of HPβCD decreased A_C (Fig. 7e) but in a lesser extent than in the case of cholesterol and SM (reduction of ~ 17% for POPC vs ~ 30% for cholesterol and SM). No effect on A_C was observed for the BUD:HPβCD complex with POPC or for either compound with PI monolayer. As for SM monolayer, HPβCD or BUD:HPβCD did not greatly affect the interfacial stability of POPC or PI monolayers (Fig. 7.f). However, while the HPβCD caused lipid desorption from the monolayer (Fig. 7.b–d-insets), the BUD:HPβCD complex increased slightly the surface pressure when injected under the POPC or PI monolayers. Insertion of budesonide and/or BUD:HPβCD into the monolayer can also occurs in these cases.

Overall, the BUD:HPBCD complex shows i) increased extent of destabilization of cholesterol monolayers and ii) adsorption into the phospholipid monolayers when compared to the free HPBCD. This might be due to i) a possible increase in affinity/efficacy of the HPβCD regarding cholesterol-containing membranes due to the presence of budesonide and/or ii) a possible insertion of budesonide into the monolayer.

4. Discussion

Membrane cholesterol has several important properties including the lateral segregation into cholesterol and sphingolipid-enriched domains known as lipid rafts [6]. These ordered domains have been shown to be essential for creating an appropriate microenvironment for signal reception and transduction. Lipid rafts are able to stabilize and cluster the receptor structures. This provides a sorting mechanism, and co-localizing receptors and cofactors thus being responsible for the fine-tuning of signal transduction [54]. Cyclodextrins and β-cyclodextrin are able to form inclusion complexes with cholesterol. They are commonly used to extract or insert cholesterol from membranes [55–58]. In addition, βCDs are also known to form inclusion complexes with several hydrophobic drugs [17,18,59,60] including budesonide (BUD).

Interestingly, clinical studies [14] showed a lower cellular toxicity of budesonide when budesonide was complexed with HPβCD. The aim of the present study was therefore to understand the potential effect of the extraction of cholesterol in lipid-raft domains in relation with regulation of the inflammatory response induced by the BUD:HPβCD complex. Thus, we characterized the interaction of BUD:HPβCD and HPβCD with lipid model membranes containing and lacking cholesterol and determined changes in biophysical membrane properties.

In model membranes containing cholesterol, we demonstrated an effect of BUD:HPβCD with cholesterol-enriched membranes leading to changes in membrane biophysical properties in agreement with cholesterol extraction, such as increased membrane fluidity and permeability, changes in lipid packing and lipid desorption from the lipid interface as well as the disruption of cholesterol-enriched raft-like liquid ordered domains. In comparison with HPβCD and except for membrane fluidity, all these effects were enhanced and/or observed earlier with the complex BUD:HPβCD.

The molecular mechanisms involved in cholesterol extraction by HPβCD and BUD:HPβCD was unknown but as demonstrated by Lopez et al. [50], the distribution of the cyclodextrins on the surface of the monolayer could play a critical role. Spontaneous cholesterol extraction on a nanosecond time scale might be related with a suitably oriented dimer. Moreover, free energy calculations reveal that the cyclodextrins have a strong affinity to bind to the membrane surface, and, by doing so, destabilize the local packing of cholesterol molecules making their extraction favorable [50].

For the model systems lacking cholesterol, the BUD:HPβCD and HPβCD caused an increase in DPH anisotropy for the lowest concentrations and the disappearance of liquid disordered/solid ordered phase separation in GUVs. The increase of membrane rigidity is surprising but can reasonably be ascribed to the formation of a relatively thick polymer layer around the phospholipid bilayers [48]. In the same line, Lopez et al. [50], reported from simulations studies, the formation of supra-molecular cyclodextrin structures on the surface of cholesterol monolayers. The mechanism of interaction of cyclodextrins with the lipid membrane is suggested to depend on the molecular ratio of cyclodextrins to lipid. Since cyclodextrins possess a greater affinity towards cholesterol when compared to phospholipids, it is possible that the observed increase in membrane rigidity observed for the lowest HPβCD:lipid ratio might reflect non-specific stabilizing cyclodextrin interaction with the surface of the cholesterol-free membrane. For higher HPβCD concentrations the increase in membrane fluidity coming back to values similar to those obtained for controls might be explained by extraction of lipids other than cholesterol, namely sphingomyelin. Moreover, at higher HPβCD concentrations, HPβCD:HPβCD interactions could be promoted in comparison with HPβCD:membrane interactions explaining why no global effect was observed on membrane fluidity. Regarding the effect on membrane phase separation, in absence of cholesterol, BUD:HPβCD affected membrane phase separation without increasing membrane permeability and affecting (or only slightly) the stability of SM, POPC or PI monolayers.

A critical question is the potential competition between budesonide and lipid for the HPβCD cavity which may occur at the interface. Focusing on the mechanism involved, the BUD:HPBCD complex induced a greater destabilization of the cholesterol monolayer without affecting HPBCD cholesterol extraction potential (Fig. 7a + inset). It resulted in an increase in surface pressure over time in monolayers composed of phospholipids. These results suggest an insertion of budesonide into the air:liquid interface, an exchange between the budesonide and cholesterol in favor of cholesterol. This could be related to the increased kinetics of membrane permeabilization to calcein induced by the BUD:HPβCD complex when compared with the HPβCD.

Altogether, the results showed that BUD:HPβCD and HPβCD can effectively induce significant changes in the composition and biophysical properties of cholesterol-enriched raft-like domains in model systems. Destabilization of these domains might explain the anti-inflammatory effect observed for the HPβCD (preliminary data), probably by modifying the lipid environment of receptors involved in inflammatory processes. The co-administration of budesonide and HPβCD might provide a higher therapeutic effect acting through complementary anti-inflammatory mechanisms. Thus HPβCD could play a critical role for administration of poorly soluble drug like budesonide by increasing cellular delivery of budesonide in vivo as well as for regulation of critical biophysical membrane properties of cholesterol-enriched domains where immune receptors are located. HPβCD can be both a targeted delivery vehicle and an anti-inflammatory agent by own.

Further studies about the modulation of the inflammatory response, focusing particularly on the relevance of lipid rafts in signal activation, are required to evaluate the mechanism involved in BUD:HPβCD and HPβCD anti-inflammatory properties.

Supplementary data to this article can be found online at http://dx.doi.org/10.1016/j.bbamem.2017.06.010.

Conflict of interest

The authors declare that they have no conflicts of interest with the contents of this article.

Author contributions

AGS and MPML wrote the manuscript and designed experiments.

JB contributed for the membrane fluidity and performed the membrane permeability assays.

GD, DC and BE prepared and characterized the BUD:HPβCD complex used in this study.

MD provided the expertise, equipment and resources to perform the surface pressure–area compression isotherms- and surface pressure–time (π-t) adsorption isotherms-measurements.

All authors discussed the results.

Transparency document

The Transparency document associate with this article can be found, in online version.

Acknowledgments

AGS thanks GD, DC and BE for the BUD:HPβCD used in this study.

AGS thanks PVDS for providing the equipment and training required for microscopy imaging.

AGS thanks Lucas Vanderavero (Agro-Bio Tech from the University of Liège – ULg) for his help with the surface pressure–area compression isotherm measurements.

M.-C. Cambier, and V. Mohymont provided dedicated technical assistance.

LCS is supported by Investigador FCT 2014 (IF/00437/2014) from Fundação para a Ciência e a Tecnologia, Portugal.

MD is Senior Research Associate for the Fonds National de la Recherche Scientifique (FRS-FNRS).

This work was supported by Walloon Region (AEROGAL).

References

[1] S.J. Singer, G.L. Nicolson, The fluid mosaic model of the structure of cell membranes, Science 175 (1972) 720–731.
[2] G. van Meer, Lipid traffic in animal cells, Annu. Rev. Cell Biol. 5 (1989) 247–275.
[3] K. Simons, E. Ikonen, Functional rafts in cell membranes, Nature 387 (1997) 569–572.
[4] G.L. Nicolson, The fluid-mosaic model of membrane structure: still relevant to understanding the structure, function and dynamics of biological membranes after more than 40 years, Biochim. Biophys. Acta 2014 (1838) 1451–1466.
[5] F.M. Goni, The basic structure and dynamics of cell membranes: an update of the Singer-Nicolson model, Biochim. Biophys. Acta 2014 (1838) 1467–1476.
[6] R. Schroeder, E. London, D. Brown, Interactions between saturated acyl chains confer detergent resistance on lipids and glycosylphosphatidylinositol (GPI)-anchored proteins: GPI-anchored proteins in liposomes and cells show similar behavior, Proc. Natl. Acad. Sci. U. S. A. 91 (1994) 12130–12134.
[7] J.D. Nickels, X. Cheng, B. Mostofian, C. Stanley, B. Lindner, F.A. Heberle, S. Perticaroli, M. Feygenson, T. Egami, R.F. Standaert, et al., Mechanical properties of nanoscopic lipid domains, J. Am. Chem. Soc. 137 (2015) 15772–15780.
[8] M.P. Besenicar, A. Bavdek, A. Kladnik, P. Macek, G. Anderluh, Kinetics of cholesterol extraction from lipid membranes by methyl-beta-cyclodextrin—a surface plasmon resonance approach, Biochim. Biophys. Acta 2008 (1778) 175–184.
[9] T. Murai, Lipid raft-mediated regulation of hyaluronan-CD44 interactions in inflammation and cancer, Front. Immunol. 6 (2015) 1–9.
[10] P. Varshney, V. Yadav, N. Saini, Lipid rafts in immune signaling: current progress and future perspective, Immunology 149 (2016) 13–24.
[11] M.G. Sorci-Thomas, M.J. Thomas, Microdomains, inflammation, and atherosclerosis, Circ. Res. 118 (2016) 679–691.
[12] T. Loftsson, M.E. Brewster, Pharmaceutical applications of cyclodextrins: basic science and product development, J. Pharm. Pharmacol. 62 (2010) 1607–1621.
[13] S.S. Jambhekar, P. Breen, Cyclodextrins in pharmaceutical formulations I: structure and physicochemical properties, formation of complexes, and types of complex, Drug Discov. Today 21 (2016) 356–362.
[14] S. Gould, R.C. Scott, 2-Hydroxypropyl-beta-cyclodextrin (HP-beta-CD): a toxicology review, Food Chem. Toxicol. 43 (2005) 1451–1459.
[15] A.J. Valente, O. Soderman, The formation of host-guest complexes between surfactants and cyclodextrins, Adv. Colloid Interf. Sci. 205 (2014) 156–176.
[16] H. Wei, C.Y. Yu, Cyclodextrin-functionalized polymers as drug carriers for cancer therapy, Biomater. Sci. 3 (2015) 1050–1060.
[17] C.S. Mangolim, C. Moriwaki, A.C. Nogueira, F. Sato, M.L. Baesso, A.M. Neto, G. Matioli, Curcumin-beta-cyclodextrin inclusion complex: stability, solubility, characterisation by FT-IR, FT-Raman, X-ray diffraction and photoacoustic spectroscopy, and food application, Food Chem. 153 (2014) 361–370.
[18] G. Dufour, W. Bigazzi, N. Wong, F. Boschini, P. de Tullio, G. Piel, D. Cataldo, B. Evrard, Interest of cyclodextrins in spray-dried microparticles formulation for sustained pulmonary delivery of budesonide, Int. J. Pharm. 495 (2015) 869–878.
[19] D. Hodgson, K. Mortimer, T. Harrison, Budesonide/formoterol in the treatment of asthma, Expert Rev. Respir. Med. 4 (2010) 557–566.
[20] I.M. Adcock, G. Caramori, P.A. Kirkham, Strategies for improving the efficacy and therapeutic ratio of glucocorticoids, Curr. Opin. Pharmacol. 12 (2012) 246–251.
[21] G. Caramori, P. Casolari, A. Barczyk, A.L. Durham, A. Di Stefano, I. Adcock, COPD immunopathology, Semin. Immunopathol. 38 (2016) 407–515.
[22] N.Z. Fabbri, E. Abib-Jr, Z.R. de Lima, Azelastine and budesonide (nasal sprays): effect of combination therapy monitored by acoustic rhinometry and clinical symptom score in the treatment of allergic rhinitis, Allergy Rhinol. (Providence) 5 (2014) 78–86.
[23] A. Rezaie, M.E. Kuenzig, E.I. Benchimol, A.M. Griffiths, A.R. Otley, A.H. Steinhart, G.G. Kaplan, C.H. Seow, Budesonide for induction of remission in Crohn's disease, Cochrane Database Syst. Rev. 6 (2015), CD000296.
[24] P.J. Barnes, Pathophysiology of allergic inflammation, Immunol. Rev. 242 (2011) 31–50.
[25] K. Basu, A. Nair, P.A. Williamson, S. Mukhopadhyay, B.J. Lipworth, Airway and systemic effects of soluble and suspension formulations of nebulized budesonide in asthmatic children, Ann Allergy Asthma Immunol 103 (2009) 436–441.
[26] G. Dufour, B. Evrard, P. de Tullio, Rapid quantification of 2-hydroxypropyl-beta-cyclodextrin in liquid pharmaceutical formulations by (1)H nuclear magnetic resonance spectroscopy, Eur. J. Pharm. Sci. 73 (2015) 20–28.
[27] T. Kinnarinen, P. Jarho, K. Jarvinen, T. Jarvinen, Pulmonary deposition of a budesonide/gamma-cyclodextrin complex in vitro, J. Control. Release 90 (2003) 197–205.
[28] P.A. Williamson, D. Menzies, A. Nair, A. Tutuncu, B.J. Lipworth, A proof-of-concept study to evaluate the antiinflammatory effects of a novel soluble cyclodextrin formulation of nebulized budesonide in patients with mild to moderate asthma, Ann Allergy Asthma Immunol 102 (2009) 161–167.
[29] E.G. Bligh, W.J. Dyer, A rapid method of total lipid extraction and purification, Can. J. Biochem. Physiol. 37 (1959) 911–917.
[30] G. Rouser, S. Fkeischer, A. Yamamoto, Two dimensional then layer chromatographic separation of polar lipids and determination of phospholipids by phosphorus analysis of spots, Lipids 5 (1970) 494–496.
[31] J. Lorent, C.S. Le Duff, J. Quetin-Leclercq, M.P. Mingeot-Leclercq, Induction of highly curved structures in relation to membrane permeabilization and budding by the triterpenoid saponins, alpha- and delta-Hederin, J. Biol. Chem. 288 (2013) 14000–14017.
[32] F. Schroeder, Y. Barenholz, E. Gratton, T.E. Thompson, A fluorescence study of dehydroergosterol in phosphatidylcholine bilayer vesicles, Biochemistry 26 (1987) 2441–2448.
[33] K.H. Cheng, J. Virtanen, P. Somerharju, Fluorescence studies of dehydroergosterol in phosphatidylethanolamine/phosphatidylcholine bilayers, Biophys. J. 77 (1999) 3108–3119.
[34] L.M. Loura, M. Prieto, Dehydroergosterol structural organization in aqueous medium and in a model system of membranes, Biophys. J. 1997 (72) (1997) 2226–2236.
[35] J.N. Weinstein, S. Yoshikami, P. Henkart, R. Blumenthal, W.A. Hagins, Liposome-cell interaction: transfer and intracellular release of a trapped fluorescent marker, Science 195 (1977) 489–492.
[36] P.I. Lelkes, Liposome Technology, CRC Press, Boca Raton, FL, 1984225–246.
[37] M.I. Angelova, S. Soléau, P. Méléard, J.F. Faucon, P. Bothorel, Preparation of giant vesicles by external AC electric fields. Kinetics and applications, in: C. Helm, M. Lösche, H. Möhvald (Eds.), Trends in Colloid and Interface Science VI, Steinkopff, 1992, pp. 127–131.
[38] D.J. Estes, M. Mayer, Giant liposomes in physiological buffer using electroformation in a flow chamber, Biochim. Biophys. Acta 2005 (1712) 152–160.
[39] N. Rodriguez, F. Pincet, S. Cribier, Giant vesicles formed by gentle hydration and electroformation: a comparison by fluorescence microscopy, Colloids Surf. B: Biointerfaces 42 (2005) 125–130.
[40] D. Wustner, Fluorescent sterols as tools in membrane biophysics and cell biology, Chem. Phys. Lipids 146 (2007) 1–25.
[41] M.G. Benesch, R.N. Lewis, R.N. McElhaney, A calorimetric and spectroscopic comparison of the effects of cholesterol and its immediate biosynthetic precursors 7-dehydrocholesterol and desmosterol on the thermotropic phase behavior and organization of dipalmitoylphosphatidylcholine bilayer membranes, Chem. Phys. Lipids 191 (2015) 123–135.
[42] A.L. McIntosh, A.M. Gallegos, B.P. Atshaves, S.M. Storey, D. Kannoju, F. Schroeder, Fluorescence and multiphoton imaging resolve unique structural forms of sterol in membranes of living cells, J. Biol. Chem. 278 (2003) 6384–6403.
[43] M.A. Soto-Arriaza, C. Olivares-Ortega, F.H. Quina, L.F. Aguilar, C.P. Sotomayor, Effect of cholesterol content on the structural and dynamic membrane properties of DMPC/DSPC large unilamellar bilayers, Biochim. Biophys. Acta 2013 (1828) 2763–2769.
[44] M. Seras, J. Gallay, M. Vincent, M. Ollivon, S. Lesieur, Cholesterol assemblies induced by octyl lgucoside: a time-resolved fluorescence study of dehydroergosterol, J. Colloid Interfaces B 167 (1994) 159–171.

[45] H. Ohvo-Rekila, B. Akerlund, J.P. Slotte, Cyclodextrin-catalyzed extraction of fluorescent sterols from monolayer membranes and small unilamellar vesicles, Chem. Phys. Lipids 105 (2000) 167–178.
[46] M. Shinitzky, Y. Barenholz, Fluidity parameters of lipid regions determined by fluorescence polarization, Biochim. Biophys. Acta 515 (1978) 367–394.
[47] R.F. de Almeida, A. Fedorov, M. Prieto, Sphingomyelin/phosphatidylcholine/cholesterol phase diagram: boundaries and composition of lipid rafts, Biophys. J. 85 (2003) 2406–2416.
[48] I. Puskas, L. Barcza, L. Szente, F. Csempesz, Features of the interaction between cyclodextrins and colloidal liposomes, J. Incl. Phenom. 54 (2006) 89–93.
[49] I. Puskas, F. Csempesz, Influence of cyclodextrins on the physical stability of DPPC-liposomes, Colloids Surf. B: Biointerfaces 58 (2007) 218–224.
[50] C.A. Lopez, A.H. de Vries, S.J. Marrink, Molecular mechanism of cyclodextrin mediated cholesterol extraction, PLoS Comput. Biol. 7 (2011) e1002020.
[51] S.L. Veatch, S.L. Keller, Seeing spots: complex phase behavior in simple membranes, Biochim. Biophys. Acta 2005 (1746) 172–185.
[52] J. Mascetti, S. Castano, D. Cavagnat, B. Desbat, Organization of beta-cyclodextrin under pure cholesterol, DMPC, or DMPG and mixed cholesterol/phospholipid monolayers, Langmuir 24 (2008) 9616–9622.
[53] M. Flasinski, M. Broniatowski, J. Majewski, P. Dynarowicz-Latka, X-ray grazing incidence diffraction and Langmuir monolayer studies of the interaction of beta-cyclodextrin with model lipid membranes, J. Colloid Interface Sci. 348 (2010) 511–521.
[54] D. Lingwood, K. Simons, Lipid rafts as a membrane-organizing principle, Science 327 (2010) 46–50.
[55] T. Irie, K. Fukunaga, J. Pitha, Hydroxypropylcyclodextrins in parenteral use. I: lipid dissolution and effects on lipid transfers in vitro, J. Pharm. Sci. 81 (1992) 521–523.
[56] Y. Ohtani, T. Irie, K. Uekama, K. Fukunaga, J. Pitha, Differential effects of alpha-, beta- and gamma-cyclodextrins on human erythrocytes, Eur. J. Biochem. 186 (1989) 17–22.
[57] H. Ohvo, J.P. Slotte, Cyclodextrin-mediated removal of sterols from monolayers: effects of sterol structure and phospholipids on desorption rate, Biochemistry 35 (1996) 8018–8024.
[58] A.E. Christian, M.P. Haynes, M.C. Phillips, G.H. Rothblat, Use of cyclodextrins for manipulating cellular cholesterol content, J. Lipid Res. 38 (1997) 2264–2272.
[59] N. Rocks, S. Bekaert, I. Coia, G. Paulissen, M. Gueders, B. Evrard, J.C. Van Heugen, P. Chiap, J.M. Foidart, A. Noel, et al., Curcumin-cyclodextrin complexes potentiate gemcitabine effects in an orthotopic mouse model of lung cancer, Br. J. Cancer 107 (2012) 1083–1092.
[60] J.E. Kim, H.J. Cho, D.D. Kim, Budesonide/cyclodextrin complex-loaded lyophilized microparticles for intranasal application, Drug Dev. Ind. Pharm. 40 (2014) 743–748.
[61] M. Eeman, G. Francius, Y.F. Dufrene, K. Nott, M. Paquot, M. Deleu, Effect of cholesterol and fatty acids on the molecular interactions of fengycin with stratum corneum mimicking lipid monolayers, Langmuir 25 (2009) 3029–3039.